Available online at www.sciencedirect.com
SCIENCE DIRECT®
Journal of Sound and Vibration 272 (2004) 643–655
JOURNAL OF SOUND AND VIBRATION
www.elsevier.com/locate/jsvi

Prediction of non-chaotic motion of the elastic system with small stiffness

C.-M. Lee[a,*], V.N. Goverdovskiy[b], S.B. Samoilenko[c]

[a] *School of Mechanical and Automotive Engineering, University of Ulsan, 29 Mugue-Dong, Nam-Gu, 680-749 Ulsan, South Korea*
[b] *Vibration Control Laboratory, Novosibirsk State Technical University, 20 Karl Marx Avenue, 630-092 Novosibirsk, Russian Federation*
[c] *Department of Physics of Non-Equilibrium Processes, Novosibirsk State University, 2 Polzunov St., 630-090 Novosibirsk, Russian Federation*

Received 7 May 2002; accepted 2 April 2003

Abstract

Dynamic stability in the large is considered subject to the vibration protecting mechanisms (VPMs) containing elastic links with "negative" stiffness. This analysis plays an important role in the estimation of an opportunity for improvement of vibration protection in the almost insuperable infra-low-frequency band employing these mechanisms. The Lyapunov largest exponent and Poincaré map of phase trajectories methods have been used with this purpose in mind. Numerical results demonstrate a visualization indicating the effectiveness of the methods in comparing stiffness control mechanisms (SCMs) of different types in terms of their predisposition to chaotic motion as well as to analyze dynamic stability of the VPMs with small (quasi-zero) stiffness. Also, the methods have been applied to predict behavior of controlled suspension mostly used for driver seats and modified with the help of the SCM. A criterion is formulated of dynamic stability of modified suspension.

1. Introduction

Some Systems are known to have behavior that cannot be predicted by methods of classical mechanics once motion has begun. These systems are chaotic. The multiple degrees-of-freedom

*Corresponding author. Tel.: +82-52-259-2851; fax: +82-52-259-1681.
E-mail addresses: cmlee@ulsan.ac.kr (C.-M. Lee), ATB@sol.ru (V.N. Goverdovskiy), samsergey@yandex.ru (S.B. Samoilenko).

0022-460X/03/$ - see front matter © 2003 Elsevier Ltd. All rights reserved.
doi:10.1016/S0022-460X(03)00390-0

systems or systems with distributed parameters can be referred to as chaotic. For instance, turbulence in the hydrodynamic systems is an example of harmful chaotic motion [1]

A few relatively simple mechanical systems have a predisposition to chaotic motion as well. At the same time, these phenomena could in certain cases be used as a helpful feature. Among them there is a wide class of elastic systems with non-adjacent stable equilibria. The theoretical concepts of motion and results of study of some systems have been published, in particular, in Refs. [2–5]. A number of similar elastic systems have been designed and applied, in the form of samples or of small-scale production, to vibration protection [6,7].

Recent research led to synthesis of a new type of elastic systems [8–10]. These results help to extend the concept about the helpful properties of elastic systems immanently predisposed to chaotic motion and seem to be important enough with respect to progress in vibration protection of a man and equipment, e.g., in transport.

This work presents comparative evaluation of immanence to chaos in the elastic systems of various types using the Lyapunov largest exponent and Poincaré map of trajectories methods. A few aspects of dynamic stability in the large are considered in autonomous and non-autonomous motion of elastic systems with variable torsion "negative" as well as small (quasi-zero) stiffness. Numerical results demonstrate that the methods allow to analyze inherent instability of elastic systems of these types and to estimate an opportunity of steady motion of a vibration protecting mechanism (VPM) containing elastic system with negative stiffness. This approach has been applied to analyze motion of pneumatic controlled suspension for a driver seat modified with the help of elastic system with variable torsion negative stiffness. A few features, being found out experimentally, of the suspension vibration in the infra-low-frequency band have been verified with these methods.

2. Subject of inquiry

Two types of elastic systems with non-adjacent stable equilibria are considered. Each system is presented in the form of a stiffness control mechanism (SCM) containing elastic link with negative stiffness. A spring or a set of springs, including additional connecting links absolutely rigid in the frequency range considered, is referred hereafter as an elastic link.

The first type of SCM is a part of a VPM shown in Figs. 1a–d [7]. Their elastic links may have specified properties moving along a straight-line path. Behavior of these elastic systems can be studied using a schematic diagram shown in Fig. 1e. Here $l_0(2-\Delta)$ is the distance between supports at initial strain state of elastic link pre-compressed in x direction, l_0 is a length of strainless "mother" element (e.g., a spring beam) of elastic link, Δ is the shortening of this link due to pre-compression, φ is an turning angle of elastic link under loading, $F(\varphi)$, in y direction.

The SCMs of the second type include elastic links with variable torsion negative stiffness. They have appropriate property in the large angular displacements of movable connecting link 1 relative to the base link 0 constrained with the elastic link as shown in Fig. 2. The SCM elastic link is a set of mother elements 1′ designed in the form of multiply unbounded thin-plated structures [11]. Supporting ends of each element are housed on the links 0 and 1. The thin plates work under combined supercritical loading: they are pre-compressed in axial direction; then, by rotation of the link 1 with the help of a drive, thin plates are loaded with the torque $M^{(a)}(\varphi)$. Here φ is the

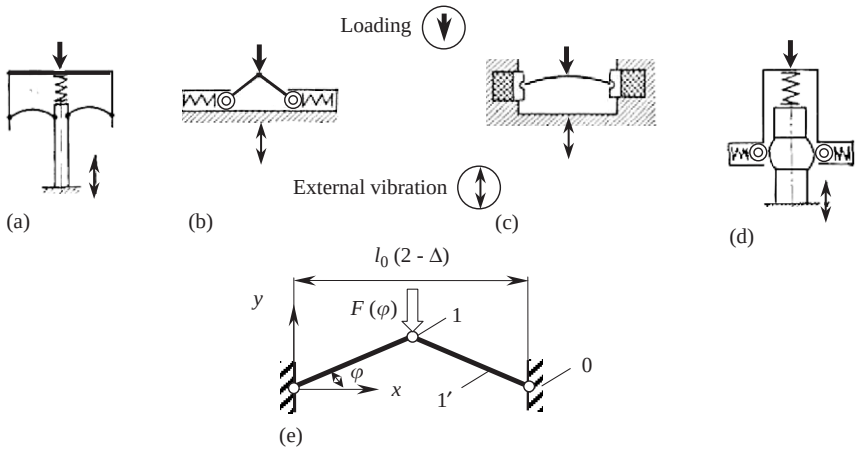

Fig. 1. VPMs containing SCMs of the first type: (a)–(d) schematic diagrams for these VPMs [7]; (e) general schematic diagram for the SCM, here are the base link (0), movable connecting links (1), and mother elements of elastic link (1′).

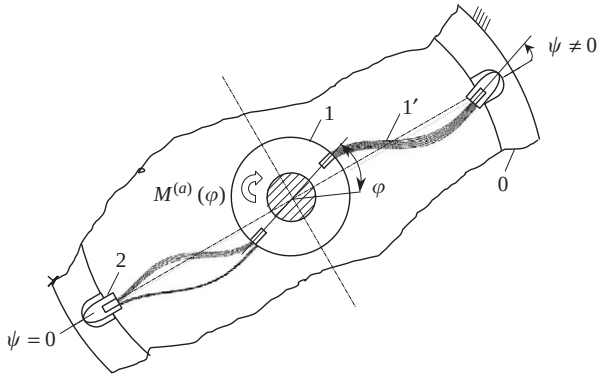

Fig. 2. A schematic diagram for SCM of the second type. Here are the base link (0), movable connecting link (1), an insertion (2), and mother elements of elastic link (1′).

angle of synchronous rotation of the link 1 and a driving link within deformation of the SCM elastic link on the segment with torsion negative stiffness. In order to eliminate lamination and, consequently, multiplicity of equilibria of the mother elements, the supporting ends of thin plates on the base link 0 are inclined by an angle ψ. The inclination range is determined from an empirical formula, $\psi = 1.08375\varphi$, under prescribed variations of pre-compression. Fig. 2 shows that the lamination takes place on periphery of φ-range if $\psi = 0$, and there is no lamination if ψ is varied. By proper ψ-variation, only the equilibrium of the SCM elastic link is kept.

It is well known that pneumatic-mechanical controlled suspensions are the most effective means among the commercial ones for vibration protection of a driver in the low and middle frequencies [12–14]. At the same time, these VPMs have inadequate effectiveness in the infra-low-frequency

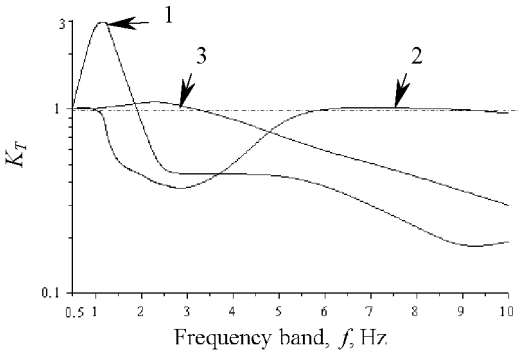

Fig. 3. Transmissibility of pneumatic-mechanical controlled suspensions. Here are the graphs 1 and 2 as in Ref. [12]; graph 3 as in Ref. [13].

band that the most harmful to human body (see Fig. 3). It was proved [10] that compact SCM of the second type can be compatible with any commercial VPM. Therefore, similar suspension used for the driver seat but modified with the help of SCM of the second type is considered as well concerning its dynamic stability in the infra-low-frequency band.

3. On the methods of investigation of chaotic motion

Those systems that are termed chaotic have by definition completely determined parameters and initial conditions in contrast to random systems. For an evaluation of dynamic stability and to predict behavior of the systems mentioned above, the Lyapunov exponents were used as the quantitative criteria of chaotic motion. The Lyapunov exponents allow measurement of the sensitivity of the system to changes in initial conditions. In other words, how fast does the system lose information about the initial state? For every dynamic process, either continuous time history or discontinuous time evolution, there is a spectrum of Lyapunov characteristic numbers indicating the expansion and contraction of initial volume of phase space under the flow or discrete mapping. However, insofar as a criterion for chaos is concerned, one needs to calculate only the largest exponent informing us of any nearby trajectories, which diverge or converge on the average [1,15].

The Lyapunov largest exponent, for a system of governing equations in the form of

$$\dot{x} = f(x) \tag{1}$$

is considered as the averaged divergence rate of nearby solutions of Eq. (1) in some test time interval. One of direct methods to calculate this rate is to assume that this divergence is locally exponential and though consider, instead of Eq. (1), variational equations

$$\dot{\eta} = \nabla f \cdot \eta, \tag{2}$$

where ∇f is the matrix of partial derivatives, $\nabla f_{i,j} = \partial f_i / \partial x_j$.

The Lyapunov largest exponent could be calculated as average increment of variation vector $\eta(t)$ during the test time interval t_{test}:

$$\Lambda = \lim_{N\to\infty} \frac{1}{Nt_{test}} \sum_{k=1}^{N} \log_2 \frac{|\eta_k(t_{test})|}{|\eta_k(0)|}. \tag{3}$$

In order to ensure maximum growth of divergence, the vector $\eta(t)$ is recalculated at each step so that its orientation tends to the direction of maximum divergence

$$\eta_k(0) = \frac{\eta_{k-1}(t_{test})}{|\eta_{k-1}(t_{test})|}. \tag{4}$$

In this case, dynamic stability of different mechanisms is described in terms of chaotic diagrams (or maps) in the parameter space. Two parameters are considered as variable: frequency and amplitude of external excitation. Using Eq. (3), the Lyapunov largest exponent is calculated for each 100×100 points in the parameter space under conditions, $N = 50$ and $t_{test} = 10$.

This method can provide reliable results during a short time and with a minimal computational burden. Computational scheme was tested subject to well-known and widely described Duffing oscillator [1,16]. In addition, these results were partially proved by analysis of the Poincaré map of attractors in the phase space and their correlation dimensions. The trajectories at some of specified points on the chaos diagrams were computed by approaches described in details, e.g., in Refs. [1,17,18].

4. Analysis of dynamic stability of the elastic systems

4.1. SCMs of the first type

Consider SCM of the first type by Fig. 1e. Stable equilibria of this system exist when

$$\varphi = \varphi_0 = \pm \cos^{-1}(1 - \Delta). \tag{5}$$

A non-dimensional governing equation of the SCM motion could be found easily, e.g., by the LaGrange method. In this case, potential energy and scaled kinetic energy of elastic system are

$$E_p = kl_0^2 \left(\frac{1 - \Delta}{\cos(\varphi)} - 1 \right),$$

$$E_k = \frac{ml_0}{3} \frac{\dot{\varphi}^2}{\tau^2} = \delta k l_0 \dot{\varphi}^2, \tag{6a, b}$$

where k is the stiffness coefficient of the SCM elastic link, m is a suspended mass, τ is the period of the system free oscillations, and also $\delta = 2\Delta(2 - \Delta)/(1 - \Delta)^2$.

Using expansion of derivative, $\partial E_p/\partial\varphi$, of potential energy by Eq. (6a), the effective stiffness of the SCM elastic link in rotation near $\varphi = \varphi_0$ could be found as $K = k\delta l_0^2$. As a time scale, the period of free oscillations is chosen in the vicinity of one of equilibria, i.e., $\tau = \sqrt{m/(3\delta k)}$.

A damping force R can be expressed as

$$R = \mu \frac{\dot{\varphi}}{\tau} = D\sqrt{3\delta}\dot{\varphi}, \tag{7}$$

where μ is the friction coefficient.

Finally, after appropriate substitutions and transformations, non-dimensional equation of free oscillations of SCM of the first type is obtained in the following form:

$$\ddot{\varphi} = F(\varphi) + D^{*}\dot{\varphi}. \tag{8}$$

Here are the balancing elastic force and scaled damping ratio, respectively:

$$F(\varphi) = \frac{1-\Delta}{\delta}\left(1 - \frac{1-\Delta}{\cos(\varphi)}\right)\frac{\sin(\varphi)}{\cos^2(\varphi)},$$

$$D^{*} = D\sqrt{3\delta}. \tag{9a, b}$$

Eq. (8), after proper substitutions, can be reduced to the equation of double-well potential Duffing oscillator if the only cubic non-linearities are left in Taylor expansion of $F(\varphi)$ in Eq. (9a).

To achieve the compatibility of results, geometrical parameters of elastic link of SCM of the first type are matched so that to hypothetically expand its control range of negative stiffness up to the range of negative stiffness of SCM of the second type in relation to angular displacements φ. Under this assumption, the force–displacement curve and the phase portrait for SCM of the first type are shown in Fig. 4a.

The analysis procedure of chaotic motion of a similar but simplified system is given in details in some publications (see, e.g., Ref. [19]). Using this approach, consider motion of SCM of the first type under a periodic external force

$$f(t) = A\mathrm{e}^{-\mathrm{j}\omega t}. \tag{10}$$

To substitute this into Eq. (8) in non-dimensional form, a normalizing factor for the amplitude A of excitation is $1/(2\delta k l_0^2)$; and frequency ω is naturally non-dimensionalized by time scale τ.

Fig. 5a shows the chaos diagram for SCM of the first type. Hereafter the shaded regions correspond to positive values of the Lyapunov largest exponent and, i.e., to chaotic phase trajectories of motion. As can be seen, the steady motion regions occupy a small part of the parameter space considered. The regions of instability continue to exist even if the frequency of excitation is increased 2–4 times. Chaotic and, respectively, unpredictable character of trajectories in the unstable motion regions leads to loss of effectiveness of the VPMs, shown in Figs. 1a–d, after the beginning of perturbation.

4.2. SCMs of the second type

A non-dimensional governing equation of motion of SCM of the second type (see Fig. 2) can be also represented in the form similar to Eq. (8).

The torque $M^{(a)}(\varphi)$, caused from a drive, is balanced by the equivalent bending moment $M(\varphi)$ due to elasticity of the SCM elastic link. It is expressed using numerical results of stress and strain states' analysis of the SCM elastic link [11]. These data can be interpolated by the polynomial of

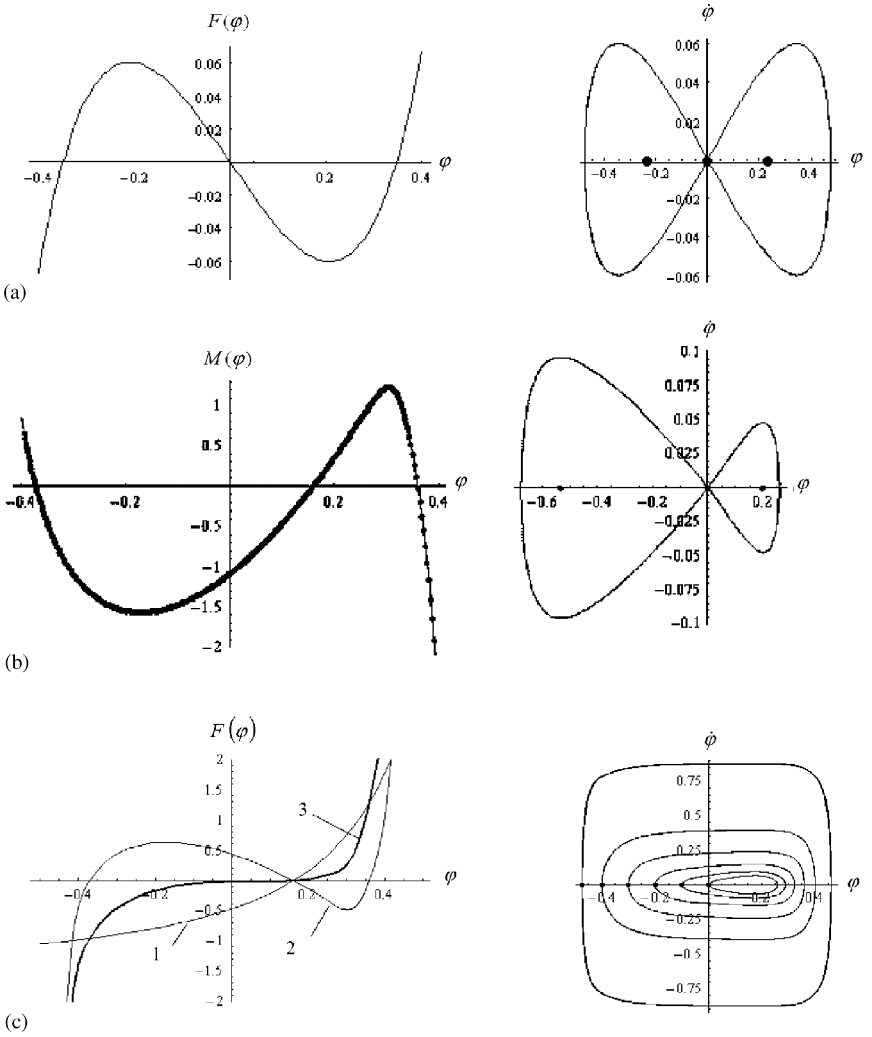

Fig. 4. Force–displacement curves and phase-portraits, respectively, for: (a) SCM of the first type; (b) SCM of the second type; (c) pneumatic-mechanical controlled suspension modified with the help of SCM of the second type.

eighth grade as

$$M(\varphi) = -0.044 + 0.21\varphi + 0.323\varphi^2 - 0.9146\varphi^3 - 5.686\varphi^4 - 19.41\varphi^5 - 33.22\varphi^6 - 182.88\varphi^7 - 84.815\varphi^8. \quad (11)$$

Non-dimensional function Eq. (11) is substituted into Eq. (8) in the following normalized form:

$$F(\varphi) = \frac{1}{\bar{k}} M(\varphi - \varphi_0), \quad (12)$$

Here the dimensionless stiffness factor, $\bar{k} = \mathrm{d}M(\varphi)/\mathrm{d}\varphi_{|\varphi=\varphi_0}$, is chosen so that the minimal frequency of free oscillations near stable equilibrium is equal to the unit; φ_0 is the semi-range of

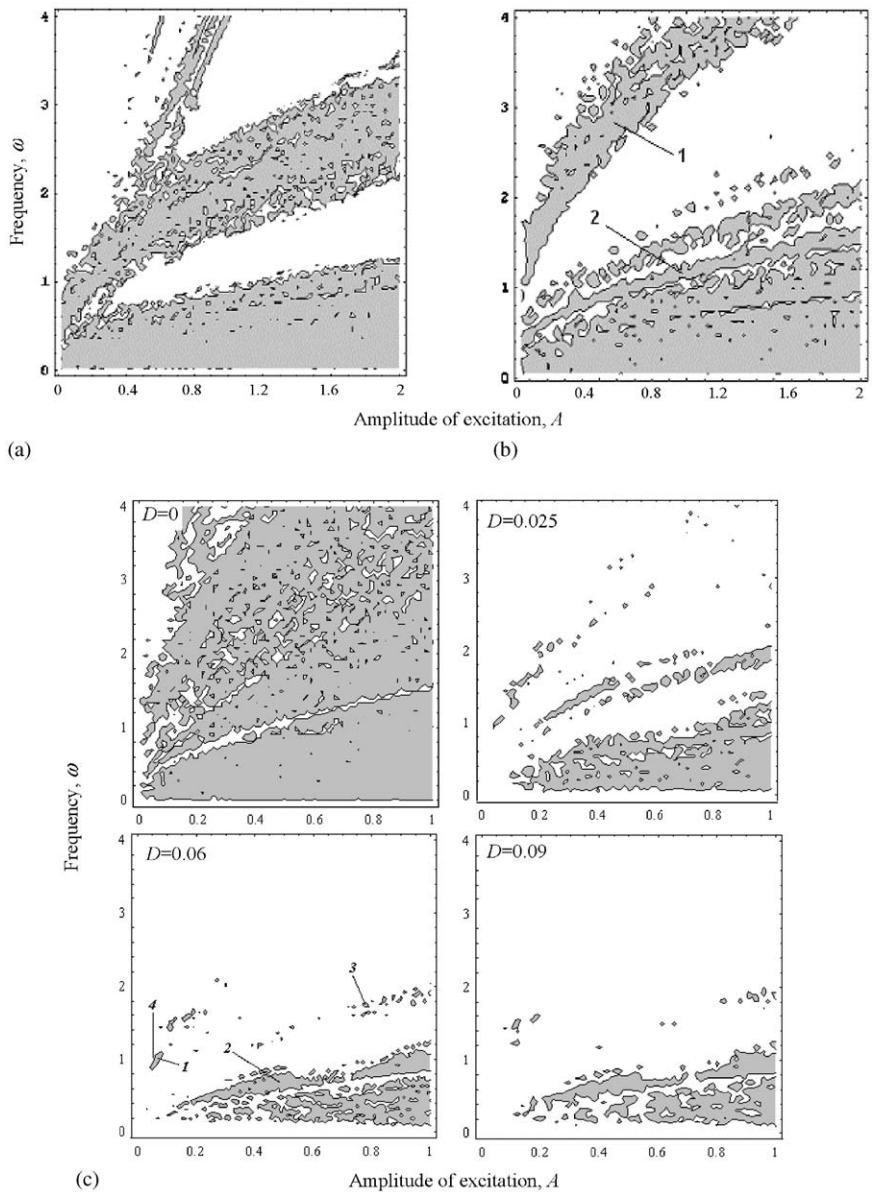

Fig. 5. Lyapunov exponent maps (chaos diagrams) for: (a) SCM of the first type; (b) SCM of the second type; (c) pneumatic-mechanical controlled suspension modified with the help of SCM of the second type, here an evolution of the suspension dynamic stability is shown depending on the damping ratio D.

reciprocal rotation of the movable connecting link 1 while the elastic link $1'$ is in a unstable equilibrium [11].

Fig. 4b shows the moment-angular displacement curve and the phase portrait for SCM of the second type. As can be seen, one of differences between SCMs of the first and second types is the asymmetry of both characteristics. But it is more important that the stiffness control range, in

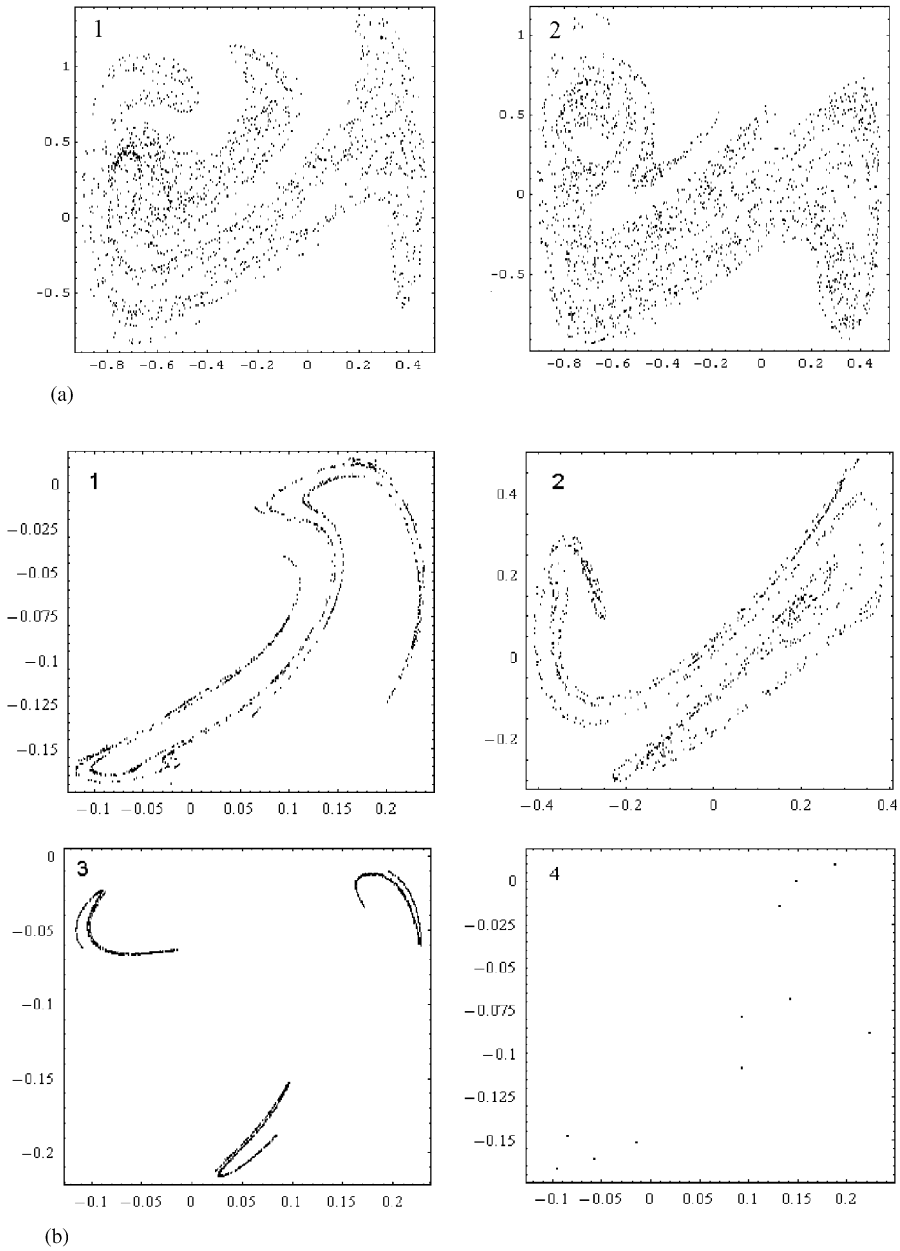

Fig. 6. Poincaré maps of trajectories constructed at: (a) the points 1 and 2 on the diagram by Fig. 5b; (b) the points 1–4 on the diagram by Fig. 5c under $D = 0.06$.

relation to angular displacements, of SCM of the second type is wider despite an attempt ad hoc to hypothetically expand similar range for SCM of the first type up to comparable value.

The Lyapunov exponent map (see Fig. 5b) confirms that motion of SCM of the second type is partly unstable in the parameter space as well. In addition, Fig. 6a shows the Poincaré maps

plotted for parameters meeting at the points 1 and 2 on the chaos diagram by Fig. 5b. Sufficiently non-integer correlation dimension of these Poincaré maps (1.17 for point 1 and 1.79 for point 2, respectively) proves the statement about chaotic character of motion. At the same time, the chaos diagram for SCM of the second type essentially differs from the corresponding diagram for the SCM by Fig. 1e. First, steady motion regions for SCM of the second type are wider and shifted to the higher frequency bands.

4.3. Pneumatic-mechanical controlled suspension modified by SCM of the second type

Consider motion of a commercial pneumatic-mechanical controlled suspension, e.g., Ref. [13]. An additional damping mechanism (hydraulic absorber [20]) is removed from kinematic chain of this suspension. At the same time, a driving link of the suspension guide mechanism is connected in parallel with movable connecting link 1 of SCM of the second type via a transmission [10].

Fig. 4c shows the averaged force–displacement curves for elastic links of the suspension modified with the help of similar SCM. Here the elastic characteristics for load-bearing elastic link (air-spring), the SCM elastic link (with variable torsion negative stiffness), and for the aggregated elastic link (with small "positive" stiffness) are shown with graphs 1–3, respectively.

For analysis of dynamic stability, the non-dimensional balancing elastic force $F(\varphi)$ is expressed as composition of the air-spring force $F_{a.-s.}(\varphi)$ and force $F_{SCM}(\varphi)$ of the SCM elastic link

$$F(\varphi) = F_{a.-s.}(\varphi) + F_{SCM}(\varphi), \tag{13}$$

where φ is the angle of synchronous reciprocal rotation of the suspension driving link and movable connecting link 1 of the SCM while its elastic link has negative stiffness.

Let us express $F_{a.-s.}$ for a simplest pneumatic air-spring that uses gas with adiabatic exponent α, and also under initial conditions in volume V_0 and pressure p_0:

$$F_{a.-s.} \propto p - p_0 = p_0\left(\left(\frac{V(\varphi)}{V_0}\right)^{-\alpha} - 1\right)$$

or

$$F_{a.-s.}(\varphi) = C\left(\frac{1}{s}(1 - s\cdot\varphi)^{-\alpha} - 1\right), \tag{14}$$

where the volume V_0 and current value, $V(\varphi)$, are expressed via the ratio s between the working stroke (segment of effective stiffness control) of modified suspension and complete vertical stroke determined from the air-spring compliance of initial suspension; C provides parameter control and, respectively, frequency turning under given conditions of the suspension form factors.

In order to scale the force $F_{SCM}(\varphi)$ with $F_{a.-s.}(\varphi)$, the function $M(\varphi)$ by Eq. (11) is normalized

$$F_{SCM}(\varphi) = \frac{M(\varphi)}{s\cdot\alpha}. \tag{15}$$

Varying parameter C, it is possible to reduce stiffness of modified suspension up to very small (quasi-zero) value in the enough expanded segment of angular displacements φ as seen from force–displacement force (Fig. 4c) that was proved experimentally [10]. The phase portrait shows that this elastic system has sufficient non-linearity, at the same time, there are not "potential wells".

Fig. 5(c) demonstrates the Lyapunov exponent maps constructed to evaluate dynamic stability of modified suspension within the damping ratio limits of $D = 0.025 - 0.09$. It was proved that the damping can be reduced up to this level if to remove an absorber. And also, steady motion of the suspension in the infra-low-frequency band is possible if damping will be of $D \in [0.025; 0.06]$ under proper stiffness control [10]. These maps indicate that motion of modified suspension is significantly more predictable (non-chaotic) then behavior of a VPM containing SCM of the first type. Here, non-dimensional frequency of excitation is normalized in the same manner as within analysis of behavior of separate SCM of the second type.

Fig. 6b additionally confirms validity of assumptions that steady motion of controlled suspension modified with the help of SCM of the second type is possible under proper stiffness control and small damping. The Poincaré maps of phase trajectories are plotted here at the points marked by numbers 1–4 on the diagram in Fig. 5c under $D = 0.06$. The points 1–3 correspond to chaotic trajectories representing strange attractor. Correlation dimensions of these maps are equal to 1.21 (point 1), 1.5 (point 2) and 1.15 (point 3), respectively, and indicate the fractal nature of trajectories. Also, point 4 lies close to point 2 but does not belong to the unstable region. The Poincaré map for point 4 shows that the trajectory, although being rather complicated, consists of a number of periodic and almost-periodic trajectories that are well-defined and are not chaotic.

Hence, the SCM of the second type has a tendency to chaotic oscillations in itself. But, being attached to a VPM, it cannot destabilize motion of the aggregate system except for the discrete infra-low frequencies. The system motion is steady including main segment in the infra-low-frequency band if $D \geqslant 0.06$. However, in the discrete frequencies dynamic stability could be lost without stiffness servo control that was predicted in Ref. [10]. Solving this special problem, assume that the force–displacement curve for the VPM has a piecewise linear segment 1, where stiffness is small but positive, and segments 2 which bound the working stroke. Instability can appear when the average values of amplitude $A(\varphi)$ are beyond segment 1 (see Fig. 7a). On segment 1, equation of motion of modified VPM can be described as following:

$$\ddot{\varphi} + D^{*}\dot{\varphi} + \bar{k}\varphi = A(\varphi)\cos[\omega t]. \tag{16}$$

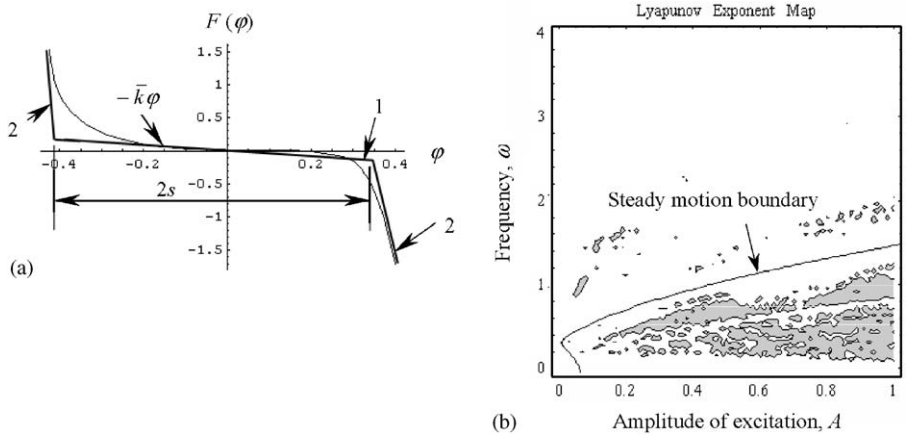

Fig. 7. On criterion of dynamic stability of pneumatic-mechanical controlled suspension modified with the help of SCM of the second type: (a) a simple piecewise linear model of the elasticity "inversion"; (b) steady motion regions.

Solution of Eq. (16) at steady state oscillations has the following form:

$$\varphi_s = A(\varphi)\frac{(\bar{k}-\omega^2)\cos(\omega t) + D^*\omega\sin(\omega t)}{\bar{k}^2 - (2\bar{k} - D^{*2})\omega^2 + \omega^4}. \tag{17}$$

The averaged amplitude of these oscillations is

$$\frac{\omega}{\pi}\int_0^{2\pi/\omega} \varphi_s^2\,\mathrm{d}t = \frac{A^2}{\bar{k}^2 - (2\bar{k} - D^{*2})\omega^2 + \omega^4}, \tag{18}$$

where φ_s is the angular displacement within limits of segment 1, i.e., within 2 s. Then the criterion of dynamic stability of modified VPM in complete infra-low-frequency band is the following:

$$\bar{k}^2 - (2\bar{k} - D^{*2})\omega^2 + \omega^4 \geqslant \frac{A^2}{s^2}. \tag{19}$$

It is remarkable that elasticity of the VPM can be inverted by servo control nearby $|\bar{k} \approx 0|$. It means that stiffness can be changed either up to positive but small value (see the curve 3 in Fig. 4c) that leads to minimum of transmissibility K_T during steady state motion or up to negative but also small value, as shown in Fig. 7a, that is adequate to the damping increasing up to critical level during a transient.

Fig. 7b shows the steady motion regions appropriating to the criterion by formula (19). There is a correlation between these results and the Lyapunov exponent calculation (see Fig. 5c under $D = 0.06$). The curvilinear line is a boundary of dynamic stability in the complete infra-low-frequency band of vibration of controlled suspension modified by SCM of the second type. The pinholes around the line mean that the small non-linearity of the elastic characteristic takes place.

5. Conclusions

The Lyapunov largest exponent and Poincaré map of trajectories methods allow to clearly compare immanent predisposition of SCMs of various types to chaotic motion. The methods can provide reliable results during a relatively short time and with a minimal computational burden. Hence, select type and design optimization of the SCMs can be more accurate using these methods.

Numerical results demonstrate a visualization and effectiveness of the methods to analyze dynamic stability as well as predict behavior of a controlled VPM modified by SCM of the second type (containing elastic links with variable torsion negative stiffness). The validity of the evaluations, done by the experiments, concerning new approaches improving vibration protection by means of SCMs has been confirmed through this study. In particular:

1. The SCM has a tendency to chaotic vibration in itself. But, being inserted into a controlled VPM, it cannot destabilize motion of aggregate elastic system.
2. Inserting the SCM into a controlled VPM and simultaneous removing an additional damper can increase mechanical Q-factor in the infra-low-frequency band though without loss of dynamic stability under conditions of small damping and proper stiffness servo control. In turn, this allows us to increase quality of vibration protection by dozens of times during steady state motion of the VPM, which is almost insuperable using a lot of well-known approaches. It

seems to be very important for men-operators and many forms of equipment operating, e.g., in transport.

3. Short-time elasticity "inversion" of SCM by the servo control near small (quasi-zero) values of stiffness can be adequate to the damping increasing up to critical level during a transient.

Acknowledgements

The authors would like to thank Prof. A.I. Temnikov (Novosibirsk Technical University, Russia) for helpful discussions. The research, which results are presented here, was carried out with the financial support of the Korean Institute of Scientific and Technical Evaluation and Planning (KISTEP, Korea).

References

[1] F.C. Moon, *Chaotic and Fractal Dynamics: An Introduction for Applied Scientists*, Wiley, New York, 1992.
[2] H. Kauderer, *Nonlinear Mechanics*, Springer, Berlin, 1961 (English edition).
[3] B. Budianski, Theory of buckling and post-buckling behavior of elastic structures, in: *Advances in Applied Mechanics*, Vol. 14, Academic Press, New York, 1974, pp. 1–65.
[4] J.G. Panovko, I.I. Gubanov, *Stability and Vibration of Elastic Systems*, 4th Edition, Nauka, Moscow, 1987 (in Russian).
[5] J.M.T. Thompson, P. Gray (Eds.), *Chaos and Dynamical Complexity in the Physical Sciences*, McGraw-Hill, London, 1990.
[6] G.S. Yurjev, *Vibration Isolation of Precision Instruments*, Russian Academy of Sciences, Siberian Branch, Institute of Nuclear Physics Press, Novosibirsk, Preprint 89-146, 1991 (in Russian).
[7] P.M. Alabuzhev, A.A. Gritchin, L.I. Kim, G.S. Migirenko, V.F. Chon, P.T. Stepanov, *Vibration Protecting and Measuring Systems with Quasi-Zero Stiffness*, Taylor & Francis, New York, 1989 (English edition).
[8] V.N. Goverdovskiy, Vibration isolating mount, Patent 1421908, Russia, 1993.
[9] V.N. Goverdovskiy, B.S. Gyzatullin, V.A. Petrov, Method of vibration isolation for the man-operator of transport-technological machine, Patent 2115570, Russia, 1998.
[10] C.-M. Lee, V.N. Goverdovskiy, Alternative vibration protecting systems for men-operators of transport machines: modern level and prospects, *Journal of Sound and Vibration* 249 (4) (2002) 635–647.
[11] C.-M. Lee, V.N. Goverdovskiy, A.I. Temnikov, Multipurpose model for synthesis of the elastic elements with torsion "negative" stiffness, in: *Proceedings of the Fifth Korean–Russian International Symposium of Science and Technology (KORUS'01)*, Russia, Tomsk, 2001, pp. 51–56.
[12] A.V. Andreytchikov, Computer modeling of creative procedures for synthesis a new in principle vibration protecting systems, *Journal of Problems in Mechanical Engineering and Reliability of Machines, Russian Academy of Sciences* 5 (1995) 89–96 (in Russia).
[13] Pneumatic controlled suspension for automotive seat, Patent 2855479, Japan, 1990.
[14] Controlled suspension of a seat, Patent 19848603, Germany, 1998.
[15] R. Seydel, *From Equilibrium to Chaos: Practical Bifurcation and Stability Analysis*, Elsevier, New York, 1988.
[16] E. Ott, *Chaos in Dynamical Systems*, Cambridge University Press, Cambridge, 1993.
[17] S. Wiggins, *Introduction to Applied Nonlinear Dynamic Systems and Chaos*, Springer, New York, 1990.
[18] J.H. Kim, J. Stringer (Eds.), *Applied Chaos*, Wiley, San Francisco, 1992.
[19] H. Clemens, J. Wauer, Free and forced vibrations of a snap-through oscillator, Report, Universität Karlsruhe, Institute für Technische Mechanik, 1981.
[20] J.Q. Sun, M.R. Jolly, M.A. Norris, Passive, adaptive and active tuned vibration absorbers: a survey, *Special Fiftieth Anniversary Design Issue, Transactions of American Society of Mechanical Engineers* 117 (1995) 234–242.